Discussion Document

Assessment of C/VM2 Return Wall Provisions
for Preventing Horizontal Fire Spread to Other Property

T.G. O'Brien
FireNZE, 2013

In completing an assessment of horizontal radiation to the boundary of other property I was surprised by the advantages of what appear to be relatively short return walls over the length of wing walls for a given exposure as specified in Table A3.1 of the Commentary to C/VM2[1].

It seems incongruous that, for a given rectangular unprotected wall perpendicular to a relevant boundary, an 0.4 m return wall could provide the same extent of radiation shielding to the boundary as a 2.5 m long wing wall.

The specific situation under assessment is shown in Figure 1 where the light blue panels represent non-fire rated radiating external walls (or openings) and the yellow panels are fire rated for the burnout duration.
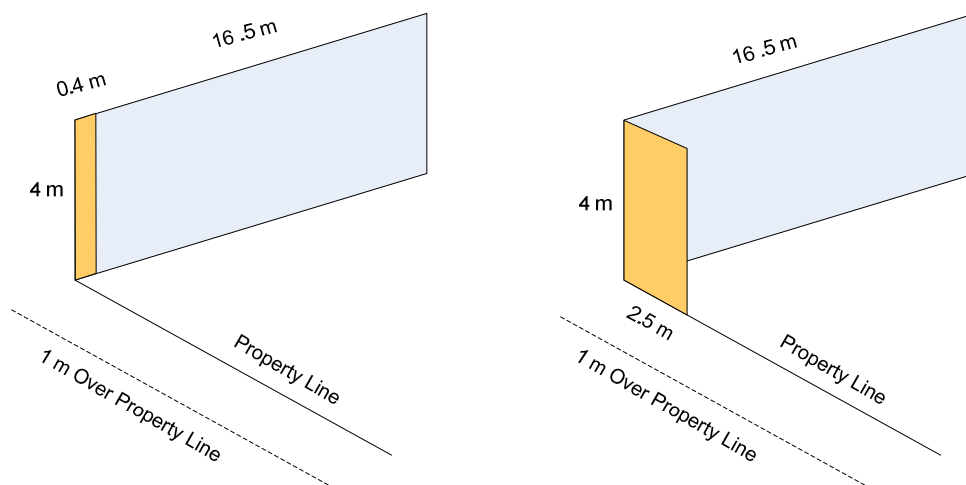

Figure 1. Situation Under Consideration

---

[1] Verification Method: Framework for Fire Safety Design For New Zealand Building Code Clauses C1-C6 Protection from Fire, effective April 2012

The limiting received radiation flux is 30 kW/m^2 at the relevant boundary and 16 kW/m^2 one metre (1 m) beyond the relevant boundary as defined in Section C3.6 of the New Zealand Building Code. These criteria do not allow for consideration of incident convective flux, or radiative and convective losses from the target elemental area.

C/VM2 design criteria specifies 144 kW/m^2 emission from exposing surfaces when the fire load energy density exceeds 800 MJ/m^2. This emission has been used throughout the following analysis.

The Building Code does not indicate whether media (air) should be considered as participating in the consideration of horizontal fire spread and makes no specific provision for radiation from flames that might project beyond the plane of the exposing unprotected element.

For the purposes of this analysis non-participating media (radiant heat transfer through a vacuum) is assumed and flame projection beyond the radiating element surface is not considered.

Using the dimensions from Figure 1, Table A3.1 allows either a 2.5 m long wing wall or an 0.4 m return wall, both specified with an adequate FRR for full burn out in an unsprinklered fire cell.

Table A3.1	Method 4 – Return walls and wing walls for unsprinklered firecells: Protection of other property																
	Return walls								Equivalent opening height h_{eq} (m)	Wing walls							
Equivalent opening height h_{eq} (m)	Minimum separation distance between *unprotected* areas and *notional boundary* D_s (m)									Minimum length of wing wall if located on the *relevant boundary* L_s (m)							
	Equivalent opening width W_{eq} (m)									Equivalent opening width W_{eq} (m)							
	1	2	3	4	6	8	10	20		1	2	3	4	6	8	10	20
1	0.4	0.4	0.4	0.4	0.4	0.4	0.4	0.4	1	0.6	0.6	0.6	0.7	0.7	0.7	0.7	0.7
2	0.4	0.4	0.4	0.4	0.4	0.4	0.4	0.4	2	0.6	0.9	1.1	1.2	1.2	1.3	1.3	1.3
3	0.4	0.4	0.4	0.4	0.4	0.4	0.4	0.4	3	0.7	1.1	1.4	1.6	1.7	1.8	1.9	1.9
4	0.4	0.4	0.4	0.4	0.4	0.4	0.4	0.4	4	0.7	1.2	1.6	1.8	2.1	2.3	2.4	2.5
6	0.4	0.4	0.4	0.4	0.4	0.5	0.5	0.5	6	0.7	1.3	1.9	2.2	2.7	3.1	3.3	4.4
8	0.4	0.4	0.4	0.4	0.4	0.5	0.5	0.7	8	0.7	1.4	2.0	2.5	3.2	3.6	5.2	6.3
10	0.4	0.4	0.4	0.4	0.5	0.6	0.7	0.9	10	0.7	1.4	2.1	2.6	3.4	4.1	6.1	7.9

Table A3.1 Commentary to C/VM2

Black body radiation transfer through non-participating media can be calculated[2] as:

$$\dot{q}_R^{''} = \Phi \varepsilon \sigma T^4 \qquad\qquad\qquad [1]$$

where $\dot{q}_R^{''}$ = received radiation flux in W/m^2

Φ = the configuration factor

ε = the emissivity of the radiator = 1

σ = the Stephan Boltzmann constant = 5.67E-8 W/m^2 K^4

T = temperature of emitter in K

σT^4 = emitted radiation flux (if specified) = 144,000 W/m^2

Black body emission and reception assumes no dependence on wavelength or angle of incidence. This is the limiting (conservative) situation for radiative heat transfer between two surfaces.

The configuration factor, sometimes called the view factor, can be calculated using an analytical (exact) solution. The relevant solution for wing and return walls is contained in the SFPE Handbook of Fire Protection Engineering, 4th Ed., Table 1.41 (and in many other references) as shown in Figure 2.

Note. There is an error in at least one of the configuration factors published in the SFPE Handbook. While the derivation of certain configuration factors for regular right and circular geometries from first principles is relatively straight forward (it is often prescribed as an undergraduate exercise) the calculations can be somewhat protracted and are therefore prone to error. The configuration factor in question (Figure 2) has been confirmed from first principles in Appendix 1.
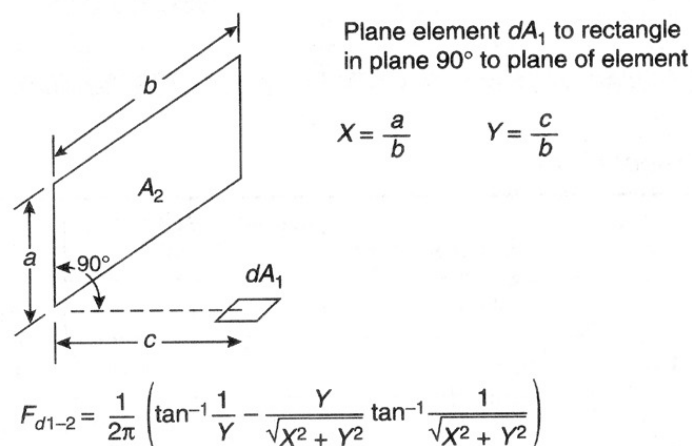

Plane element dA_1 to rectangle in plane 90° to plane of element

$$X = \frac{a}{b} \qquad Y = \frac{c}{b}$$

$$F_{d1-2} = \frac{1}{2\pi}\left(\tan^{-1}\frac{1}{Y} - \frac{Y}{\sqrt{X^2+Y^2}}\tan^{-1}\frac{1}{\sqrt{X^2+Y^2}}\right)$$

Figure 2. Analytical Solution to Configuration Factor

---

[2] Drysdale, D., 'An Introduction to Fire Dynamics', 2nd Ed., Section 2.4.1, J. Wiley & Sons, 1998

By considering the geometry and symmetry of Figure 1 the full configuration factor can be calculated by 'configuration factor algebra' involving the subtraction and addition of several sub-configuration factors as shown in Figure 3. Each of these sub-configuration factors takes the general geometric relationship shown in Figure 2 allowing for direct analytical solutions.
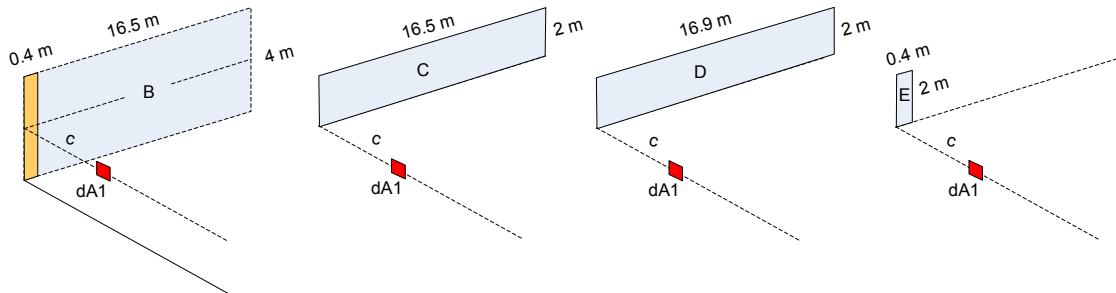

Figure 3. Configuration Factor Algebra

So for a wing wall, the configuration factor is:

$$F_{dA1-W} = 2\ F_{dA1-C} \qquad\qquad [2]$$

where: W is the total area of the unprotected wall in m^2

dA1 is an element of area at a distance c (in m) from the wall, and perpendicular to both the wall and the plane of symmetry (indicated with dashed lines).

And for a return wall:

$$F_{dA1-B} = 2\ (F_{dA-D} - F_{dA-E}) \qquad\qquad [3]$$

where: B is the total area of the unprotected wall in m^2

The solution to the incident radiation flux in Figure 1 was solved using Equations [1] to [3] and the configuration factor of Figure 2 with Microsoft Excel. As a consequence of symmetry the maximum received radiation flux will occur on the line of intersection of the horizontal plane through the centreline of the radiating unprotected area and the vertical plane through the boundary.

The calculated maximum received radiation flux is shown graphically in Figure 4 as a function of the distance c from the radiating unprotected element.
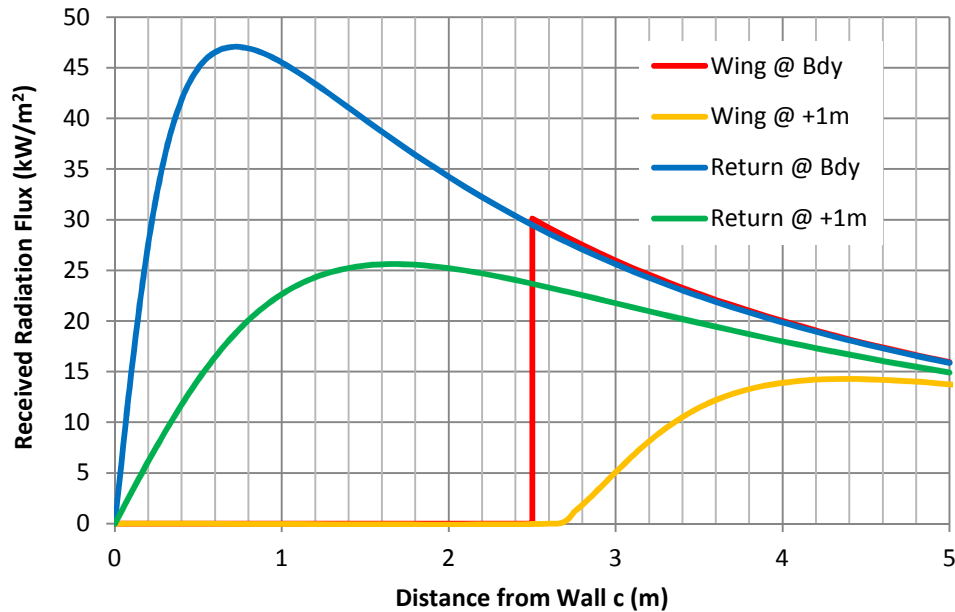
Figure 4. Received Radiation Flux at Distance c from Wall
(Analytical Result)

It is immediately apparent from Figure 4 that:

1. a 2.5 m long wing wall does not comply with a maximum received radiation flux of 30 kW/m^2 at the relevant boundary. The red curve is just above 30 kW/m^2 at a distance of 2.5 m from the wall.

2. a 2.5 m long wing wall will comply with the with a maximum received radiation flux of 16 kW/m^2 1 m beyond the relevant boundary. The orange curve remains below 16 kW/m^2.

3. an 0.4 m long return wall will not meet the specified radiation requirements at the relevant boundary or 1 m beyond the relevant boundary. The blue curve exceeds 30 kW/m^2 and the green curve exceeds 16 kW/m^2.

It is instructive to also consider the case of an unprotected wall perpendicular to and on the boundary (the zero length wing or return wall case). Figure 5 shows the limiting behaviour for received radiation flux on the boundary.
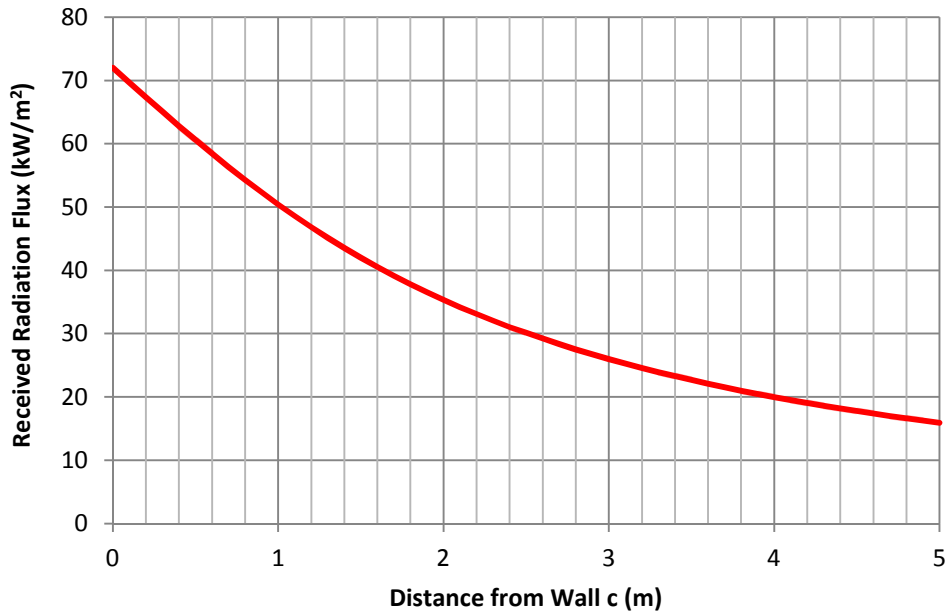
Figure 5. Zero Length Wing or Return Wall at the Relevant Boundary
(Analytical Result)

The maximum received radiation flux at the intersection of the wall and the boundary (c=0) is 72 kW/m^2 in accordance with the limit established in Appendix A Equation [44].

FDS Simulations

Short of running actual fire tests to confirm the analytical results, a number of simple experiments were modelled in Fire Dynamics Simulator[3] 5.5.3 (FDS) using the geometries from Figure 1.

Details of the simulation, sensitivity analysis and results are contained in Appendix B.

Note that it is not necessary to incorporate obstructions to represent return walls in the models. More information can be gained by establishing the unprotected wall geometry relevant to the receiving plane of interest and mapping the received radiation flux over that plane.

---

[3] Fire Dynamics Simulator, National Institute of Standards and Technology (NIST), US Department of Commerce

The models were run for a total of five simulation seconds to allow the FDS numerical computation to fully stabilise. Received radiation flux was captured as a BOUNDARY quantity and point measurements were taken from an array of radiometer DEVICES.

Simulation Results

The unprotected wall (coloured red in Figure 6) produced a heat flux of 144 kW/m^2 into the domain in all models.

Received radiation flux fields were symmetric about the centreline of the radiating panel.

Asymptotic behaviour was in accordance with the analytical results (refer to Appendix A, Equations [44] and [45]).

Fringing effects were evident, emanating from the corners, and upper and lower edges of the radiating panel. These were determined to be a consequence of the computational limits of solid angle resolution at acute angles. Although fringing effects can be reduced through increased mesh and solid angle resolution, this model refinement comes with a significant increase in computational burden and no appreciable benefit on the modelled maximum received radiation flux.
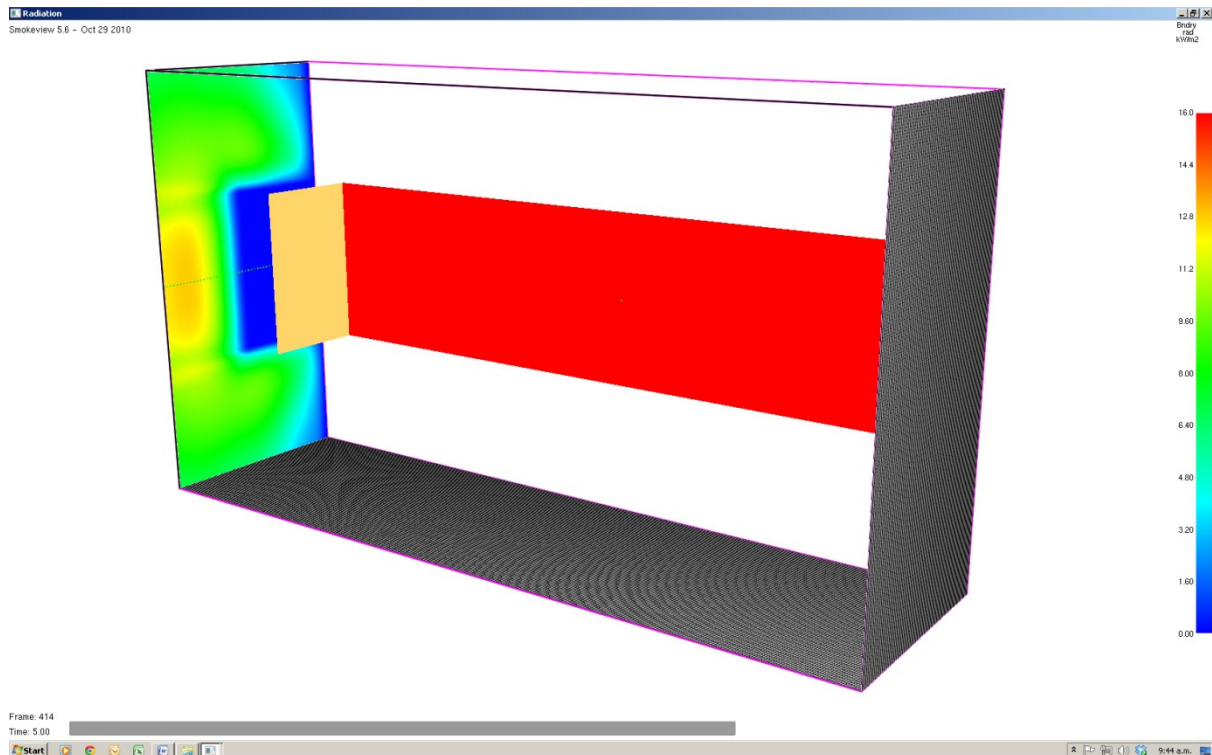

Figure 6. Wing Wall Model of Received Radiation Flux 1 m Beyond
the Relevant Boundary (showing computational grid)

Error Analysis

Both the analytical and modelled data are deterministic (not subject to random variation) hence statistical measures of 'goodness of fit' are not strictly applicable or cannot be calculated, and in any case are of questionable value[4]. However:

> The modelled received radiation flux in Figures 7 and 8 are within 1.8 kW/m^2 of the analytical results shown in Figures 4 and 5 for all simulations at all distances, c.

> The greatest variance between modelled and analytical curves was 0.19 kW^2/m^4 for the return wall case.

> The greatest Mean Absolute Deviation between modelled and analytical curves was 0.8 kW/m^2 for the no wing/return wall case shown in Figures 5 and 8.

Qualitatively the FDS modelled results are so similar to the analytical solutions that they can be considered identical for the purposes of this study. Overlays of the analytical results and the FDS simulations are provided in Appendix C to facilitate qualitative visual examination.

It can be concluded that the FDS models validate both the analytical configuration factor of Figure 2 and its Microsoft Excel implementation for all of the situations of interest.
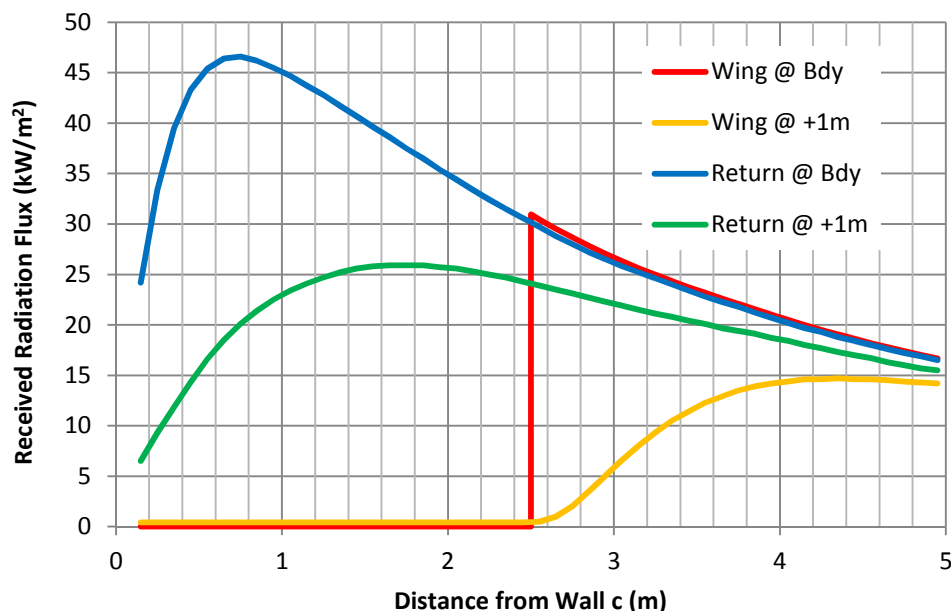

Figure 7. FDS Models of Received Radiation at
Distance c from the Perpendicular Wall

---

[4] Schunn, C. D., and Wallach, D., 'Evaluating Goodness-of-Fit in Comparison of Models to Data', University of Pittsburgh, 2001
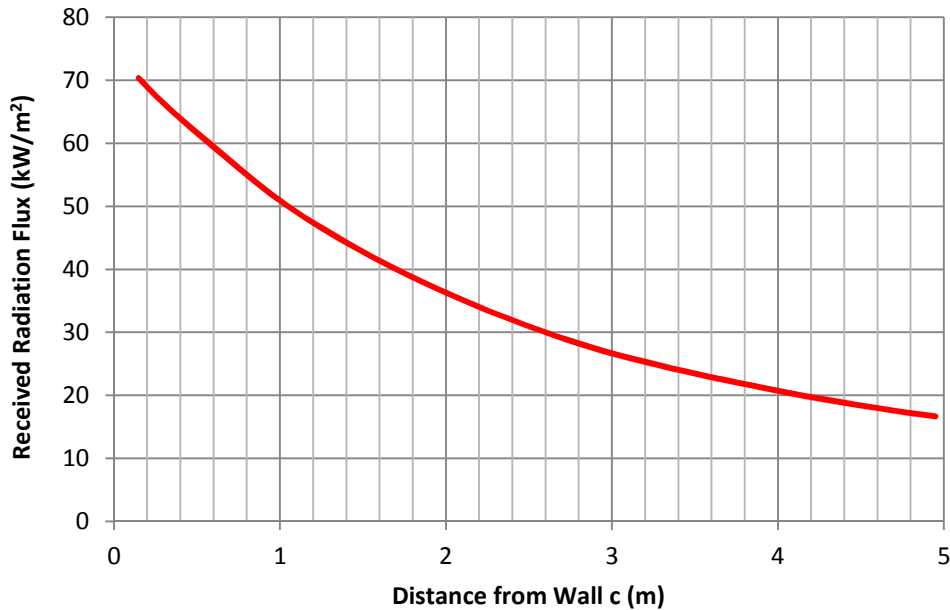
Figure 8. FDS Model of Radiation at the Relevant Boundary from a Zero Length Wing or Return Wall at the Relevant Boundary

FireWind Radiation Calculator

The radiation calculator, RADIATION, in the program suite FireWind[5] (here-in-after referred to simply as FireWind) is often used as the basis for determining radiation at and beyond the relevant boundary for the purposes of establishing compliance with the requirements of the New Zealand Building Code.

The program uses numerical integration to solve the analytical solution for received radiation flux <u>on a plane normal to the maximum received radiation flux vector</u> from up to 20 rectangular radiators in planes parallel to the X, Y and/or Z Cartesian axes.

The underlined functionality is clearly stated in the FireWind Users' Manual:

> The receptor which is of interest is usually an opening of a building adjacent to a building on fire. However, a combustible item, for instance, a curtain, can have orientation quite different from the plane of this opening. Hence, it is of interest to find the heat flux impressed on a receptor of such an orientation which corresponds to the maximum heat flow.

This is illustrated diagrammatically in Figure 9, however this simplified diagram extends to three dimensions in practice.

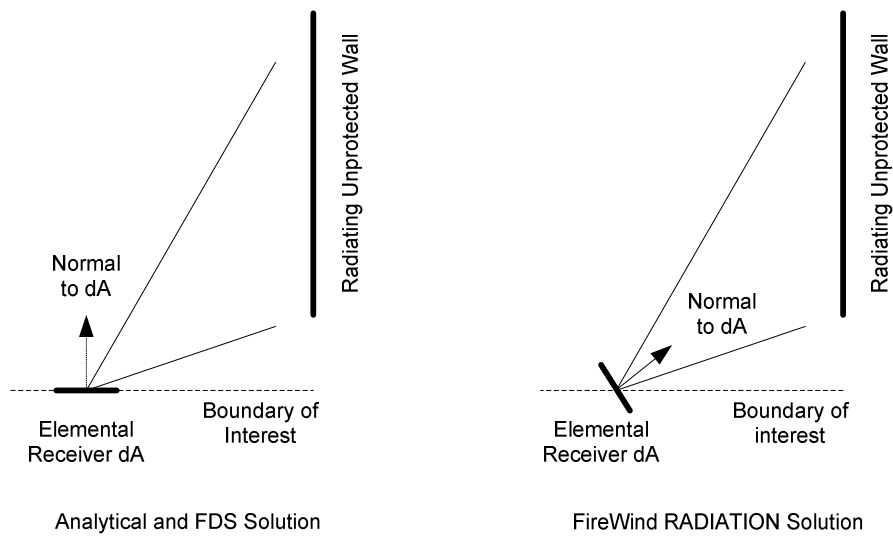[5] FireWind 3.6, Fire Modelling and Computing, NSW, Australia, Version 20, 2013

Figure 9. The Fundamental Difference Between FireWind and the Analytical
Calculation is the Orientation of dA

The consequence of the direction of the normal vector in FireWind is a higher received radiation flux than at a receiving elemental area in a right perpendicular plane to the radiating element for an otherwise identical model. The exception is the limiting behaviour when the radiating element is viewed within an acute solid angle. This occurs as the elemental area approaches the plane of the radiating element. In this limiting case the two normal vectors to the elemental areas become progressively collinear and the FireWind calculated radiation flux approaches the perpendicular case from above.

Comparative results of FireWind and analytical calculations on the line of intersection of the horizontal plane through the centreline of the radiating unprotected area and the vertical plane through the boundary are shown in Figures 10 and 11. For completeness details of the FireWind input and spatial output for these studies are contained in Appendix D.
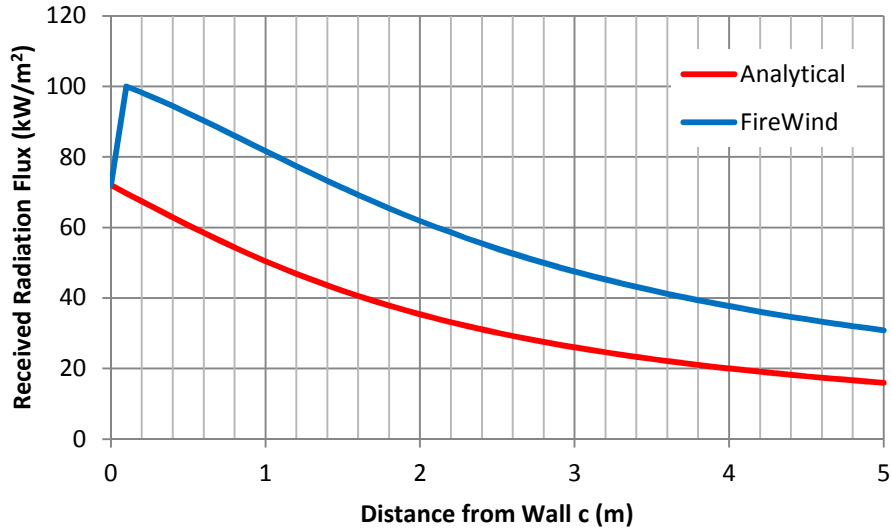
Figure 10. FireWind Model of Radiation at the Relevant Boundary from a Zero Length Wing or Return Wall at the Relevant Boundary
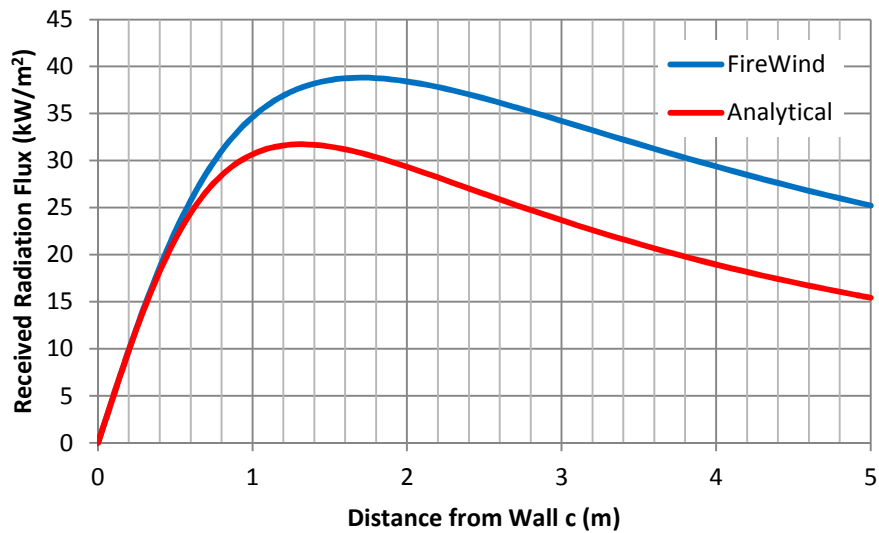

Figure 11. FireWind Model of Radiation 1 m Beyond the Relevant Boundary from a Zero Length Wing or Return Wall at the Relevant Boundary

The requirements of the NZBC for horizontal fire spread to other property are embodied in Clauses C3.6 and C3.7.

C3.6 *Buildings* must be designed and constructed so that in the event of *fire* in the building the received radiation at the *relevant boundary* of the property does not exceed 30 kW/m² and at a distance of 1 m beyond the relevant boundary of the property does not exceed 16 kW/m².

C3.7 External walls of *buildings* that are located closer than 1 m to the *relevant boundary* of the property on which the *building* stands must either:

(a) be constructed from materials which are not *combustible building materials*, or

(b) for *buildings* in importance levels 3 and 4, be constructed from materials that, when subjected to a radiant flux of 30 kW/m², do not ignite for 30 minutes, or

(c) for *buildings* in Importance Levels 1 and 2, be constructed from materials that, when subjected to a radiant flux of 30 kW/m², do not ignite for 15 minutes.

The received radiation flux criteria of Clause C3.6 is defined *at the relevant boundary*. This definition is open to interpretation because it does not state explicitly whether the received radiation flux should be assessed normal to the plane of the boundary or normal to the vector of maximum radiation incidence.

The interpretation 'normal to the plane of the boundary' is assumed because Clause C3.6 does not require consideration of '*maximum received radiation flux*', and does not reference any specific building element. This interpretation is supported by the definition of intersection angle in Appendix A, A1.0 of the Commentary to C/VM2.

While the computational implementation of the view factor and numerical accuracy of FireWind have not been validated by this analysis, a review of publications by Shestopal[6] and Lie[7] indicate the validity of the underlying methodology. A literature search did not identify published validation of the software.

Validation aside, FireWind can be expected to produce conservative results for assessing horizontal fire spread to other property in accordance with the New Zealand Building Code criteria. When used for the purposes of design, FireWind is likely to require excessively large protection features and/or boundary separations, with associated construction cost, and both site-layout and amenity repercussions.

Tabular Corrections

The analytical solution to the configuration factor was applied to the geometry specified in Table A3.1 of the Commentary to C/VM2 for both received radiation flux at the boundary and one metre beyond the boundary. The merged tabular results rounded up to the nearest 0.1 m are presented in Table 1.

---

[6] Shestopal, V. O., 'Computer Modelling of Heat Radiation from Several Emitters with Applications', Intl. Journal on Engineering Performance Based Fire Codes, Vol. 4, No. 4. Pp 112-118, 2002

[7] Lie, T. T., 'Fire and Building', Applied Science Publishers Limited, London, 1972

Return Walls									Wing Walls								
Equivalent opening height heq (m)	Minimum distance between unprotected areas and notinal boundary Ds (m)								Equivalent opening height heq (m)	Minimum length of wing wall if located on the relevant boundary Ls (m)							
	Equivalent opening width Weq (m)									Equivalent opening width Weq (m)							
	1	2	3	4	6	8	10	20		1	2	3	4	6	8	10	20
1	0.3	0.3	0.3	0.3	0.3	0.3	0.3	0.3	1	0.5	0.6	0.7	0.7	0.7	0.7	0.7	0.7
2	0.4	0.5	0.5	0.6	0.6	0.6	0.6	0.6	2	0.7	1.0	1.1	1.2	1.3	1.3	1.3	1.3
3	0.4	0.6	0.7	0.8	0.8	0.9	0.9	1.0	3	0.7	1.2	1.4	1.6	1.8	1.9	1.9	2.0
4	0.5	0.7	0.9	1.0	1.2	1.4	1.4	1.6	4	0.7	1.3	1.6	1.9	2.2	2.3	2.4	2.6
6	0.5	0.9	1.3	1.6	2.0	2.2	2.4	2.8	6	0.8	1.4	1.9	2.3	2.8	3.1	3.3	3.9
8	0.5	1.1	1.6	2.0	2.6	2.9	3.2	3.8	8	0.8	1.4	2.0	2.5	3.2	3.7	4.0	5.4
10	0.5	1.2	1.9	2.4	3.1	3.6	3.9	4.8	10	0.8	1.5	2.1	2.6	3.5	4.1	4.6	6.7

DO NOT INTERPOLATE

Table 1. Revised Return and Wing Wall Requirements
based on Analytical Calculation of Received Radiation Flux at
and 1 m Beyond the Relevant Boundary

It should be noted that while received radiation flux is a 'well behaved' function it is not linear. Interpolation between tabular values should not be permitted (contrary to the note to Table 7.3 of the former C/AS1, Amendment 5, 1 October 2005) as this can result in excessive received radiation flux at the boundary for certain cases.

There are significant discrepancies between the entries of Table 1 and Table A3.1. The entries in Table A3.1 that result in received radiation flux exceeding the New Zealand Building Code criteria are highlighted in Table 2.

Table A3.1	Method 4 – Return walls and wing walls for unsprinklered firecells: Protection of other property																
	Return walls									Wing walls							
Equivalent opening height h_{eq} (m)	Minimum separation distance between *unprotected areas* and *notional boundary* D_s (m)								Equivalent opening height h_{eq} (m)	Minimum length of wing wall if located on the *relevant boundary* L_s (m)							
	Equivalent opening width W_{eq} (m)									Equivalent opening width W_{eq} (m)							
	1	2	3	4	6	8	10	20		1	2	3	4	6	8	10	20
1	0.4	0.4	0.4	0.4	0.4	0.4	0.4	0.4	1	0.6	0.6	0.6	0.7	0.7	0.7	0.7	0.7
2	0.4	0.4	0.4	0.4	0.4	0.4	0.4	0.4	2	0.6	0.9	1.1	1.2	1.2	1.3	1.3	1.3
3	0.4	0.4	0.4	0.4	0.4	0.4	0.4	0.4	3	0.7	1.1	1.4	1.6	1.7	1.8	1.9	1.9
4	0.4	0.4	0.4	0.4	0.4	0.4	0.4	0.4	4	0.7	1.2	1.6	1.8	2.1	2.3	2.4	2.5
6	0.4	0.4	0.4	0.4	0.4	0.5	0.5	0.5	6	0.7	1.3	1.9	2.2	2.7	3.1	3.3	4.4
8	0.4	0.4	0.4	0.4	0.4	0.5	0.5	0.7	8	0.7	1.4	2.0	2.5	3.2	3.6	5.2	6.3
10	0.4	0.4	0.4	0.4	0.5	0.6	0.7	0.9	10	0.7	1.4	2.1	2.6	3.4	4.1	6.1	7.9

Table 2. Table A3.1 from Commentary to C/VM2 with
Non-Compliant Discrepancies Highlighted

The reasons for the discrepancies are not apparent. While Table A3.1 is a direct copy of the Fire Hazard Category 3 and 4 requirements of Table 7.3 of the former C/AS1, Amendment 5, 1 October 2005, it is not clear how these tabular values were originally calculated or validated.

Many of these discrepancies could be attributed to rounding, however many cannot. If the discrepancies were due to rounding errors then rounding has exceeded typical construction tolerances (as defined by ISO 3443-5:1982).

Return or wing wall thickness might also explain some discrepancies but this conjecture is not supported by either the requirements of the former Acceptable Solution (which would be expected to have specified a minimum return or wing wall thickness) or a pattern of discrepancies that could be attributed to such a cause.

While non-highlighted values of Table 2 do not exceed the received radiation flux requirements of the Building Code many are overly conservative resulting in excessively large protection features or boundary separations, with associated construction cost, and both site-layout and amenity repercussions.

Conclusions

The conclusions of this discussion document are that:

1.   the tabular solutions in Table A3.1 of the Commentary to C/VM2 are not consistent with analytical (exact) calculations of received radiation flux at and one metre beyond the relevant boundary as established in the New Zealand Building Code. Other tabular entries comply but may be overly conservative for a specified geometry.

2.   FDS, with the selection of appropriate mesh and solid angle resolution, provides a useful tool for assessment of received radiation flux at a specified boundary, particularly for complex geometries. While analytical solutions may provide optimum wing or return wall dimensions from which compliance can be determined, analytical solutions do not exist for many real world situations.

3.   FireWind will conservatively overstate the received radiation flux at a boundary as the program calculates incident radiation on the plane normal to the maximum received radiation flux vector. While this ensures compliance with the requirements of the Sections C3.6 and 7 of the Building Code it may result in excessive clearance or protection by fire rated elements when used as a design tool.

Recommendations

It is recommended that:

1.   the tabular solutions in Table A3.1 of the Commentary to C/VM2 should be corrected to comply with the minimum requirements specified in Clause C3.6 of the New Zealand Building Code 2004.

2.   the definition of what constitutes received radiation flux for the purposes of the New Zealand Building Code horizontal fire spread should be clarified.

3.   when tabular entries for wing or return walls are too restrictive for a particular design analytical solutions should be applied when available.

4.   when analytical solutions are not available, and as an acceptable alternative design methodology, CFD computational analysis of radiation to, and beyond, the relevant boundary should be accepted as evidence of compliance. CFD studies should be subject to sensitivity analysis of the mesh dimensions and solid angle resolution, perhaps through consideration of simplified geometries where analytical solutions exist.

5.   subject to validation, the RADIATION program in the suite FireWind provides a conservative method of determining compliance with the minimum requirements for New Zealand Building Code. However the use of RADIATION as a design tool is likely to result in overly conservative protective measures.

6.   the relevant government department should consider how this matter might be addressed for existing buildings where horizontal fire spread to other property has been based on existing tabular solutions.

Appendix A

Derivation of Configuration Factor

I was rather hoping to avoid completing this derivation from first principles by finding an equivalent calculation in one of the many texts on heat transfer theory. The few derivations that I found contained 'leaps of faith' from one step to the next and several had mistakes in the calculus. Most simply stated the configuration factor and left the derivation as a 'suggested exercise' for reader.

The following derivation is perhaps not as rigorous as some might like (I am certain to left off limits that apply to certain functions) and there are limitations to the extent of the underlying mathematics that I cannot reasonably describe here. This discussion document is not intended to be a dissertation on the calculation of configuration factors or a treatise on the Calculus. However, with the help of a good undergraduate calculus text[8] and a basic knowledge of trigonometry you should be able to follow the essence of the derivation. And then you can revert to using published configuration factors knowing why you don't want to derive them from first principles.

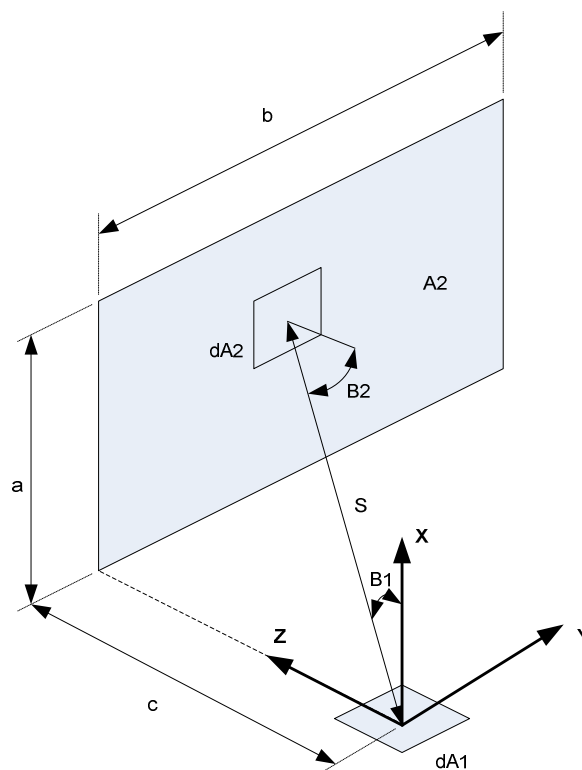Consider the geometry of the problem under consideration at Figure A1.

Figure A1. Problem Geometry

[8] Anton, H., 'Calculus with Analytical Geometry', 2nd Ed., J. Wiley & Sons, 1984

The configuration factor looking from elemental area dA_1 to A_2 is defined [9] as:

$$F_{d1-2} = \oint \frac{Cos\beta_1 Cos\beta_2}{\pi s^2} dA_2 \qquad [1]$$

From the geometry of the problem:

$$Cos\beta_1 = \frac{x}{s} \qquad [2]$$

$$Cos\beta_2 = \frac{z}{s} \qquad [3]$$

and $\quad s^2 = x^2 + y^2 + z^2 \qquad [4]$

Letting

$$dA_2 = dx\, dy$$

and substituting [2] and [3] into [1] gives:

$$F_{d1-2} = \int_0^b \int_0^a \frac{\frac{z}{s}\frac{x}{s}}{\pi s^2}\, dx\, dy \qquad [5]$$

$$= \int_0^b \int_0^a \frac{z\,x}{\pi s^4}\, dx\, dy$$

Now substituting [4] into [5], moving constants to the left of the integrals gives:

$$F_{d1-2} = \frac{z}{\pi} \int_0^b \int_0^a \frac{x}{(x^2 + y^2 + z^2)^2}\, dx\, dy \qquad [6]$$

To solve the inner integral we use the substitutions:

$$q^2 = y^2 + z^2 \qquad [7]$$

and

$$u = x^2 + q^2 \qquad [8]$$

Differentiating [8] directly with respect to x gives:

$$\frac{du}{dx} = 2\,x$$

And rearranging:

$$\frac{du}{2} = x\, dx \qquad [9]$$

Substituting [8] and [9] into [6] gives:

---

[9] Reference to underlying geometry

$$F_{d1-2} = \frac{z}{\pi} \int_0^b \int_0^* \frac{1}{2} \frac{1}{u^2} \, du \, dy \qquad [10]$$

Where the upper limit of the inner integral (from [8]) is:

$$* = a^2 + q^2 \qquad [11]$$

Moving the constant ½ outside the integrals gives:

$$F_{d1-2} = \frac{z}{2\pi} \int_0^b \int_0^* \frac{1}{u^2} \, du \, dy \qquad [12]$$

Solving the inner integral directly gives:

$$F_{d1-2} = \frac{z}{2\pi} \int_0^b \left| \frac{1}{-u} + C \right|_0^* dy \qquad [13]$$

Substituting [8] and [11] into [13] gives:

$$F_{d1-2} = \frac{z}{2\pi} \int_0^b \left| \frac{1}{-(x^2+q^2)} + C \right|_0^a dy \qquad [14]$$

And solving the definite integral:

$$F_{d1-2} = \frac{z}{2\pi} \int_0^b \left(\frac{1}{-(a^2+q^2)} + C - \frac{1}{-q^2} - C \right) dy \qquad [15]$$

$$= \frac{z}{2\pi} \int_0^b \left(\frac{1}{q^2} - \frac{1}{(a^2+q^2)} \right) dy$$

$$= \frac{z}{2\pi} \int_0^b \left(\frac{1}{q^2} - \frac{1}{(a^2+q^2)} \right) dy$$

Now substitute [7] into [15]:

$$F_{d1-2} = \frac{z}{2\pi} \int_0^b \left(\frac{1}{y^2+z^2} - \frac{1}{(a^2+y^2+z^2)} \right) dy \qquad [16]$$

The two addends in the remaining integrand can be separated:

$$F_{d1-2} = \frac{z}{2\pi} \left[\int_0^b \left(\frac{1}{y^2+z^2} \right) dy - \int_0^b \left(\frac{1}{(y^2+a^2+z^2)} \right) dy \right] \qquad [17]$$

Each of the integrands are an identity which, for the sake of clarity, is derived in equations [18] to [35] as follows.

Let $\quad y = \tan^{-1}(x) \quad$ where $|x| < \pi/2$ $\qquad [18]$

so $\quad x = \tan(y)$ $\qquad [19]$

Differentiating directly with respect to y:

$$\frac{dx}{dy} = \sec^2(y) \qquad [20]$$

and taking reciprocals:

$$\frac{dy}{dx} = \frac{1}{\sec^2(y)} \tag{21}$$

Now substituting [18] we have:

$$\frac{dy}{dx} = \frac{1}{\sec^2(\tan^{-1}(x))} \tag{22}$$

We need a trigonometric identity for the denominator:

$$\cos^2\theta + \sin^2\theta = 1 \tag{23}$$

Dividing by $\cos^2\theta$:

$$1 + \tan^2\theta = \sec^2\theta \tag{24}$$

Now let $\theta = \tan^{-1}(x)$. Substituting into [24]:

$$1 + \tan^2(\tan^{-1}(x)) = \sec^2(\tan^{-1}(x)) \tag{25}$$

so

$$1 + x^2 = \sec^2(\tan^{-1}(x)) \tag{26}$$

And substituting into [22]:

$$\frac{dy}{dx} = \frac{1}{1+x^2} \tag{27}$$

From [18], $y = \tan^{-1}(x)$ so:

$$\frac{d(\tan^{-1}(x))}{dx} = \frac{1}{1+x^2} \tag{28}$$

Taking integrals of both sides we have:

$$\int \frac{d(\tan^{-1}(x))}{dx} dx = \int \frac{1}{1+x^2} dx \tag{29}$$

$$\tan^{-1}(x) + C = \int \frac{1}{1+x^2} dx$$

where C is a constant of integration.

The general form of the integrals of equation [17] is:

$$\int \frac{1}{x^2 + a^2} dx \tag{30}$$

where a is a constant.

This is similar to [29] and can be solved using substitution.

Let:

$$x = a\,u \qquad\qquad [31]$$

so $\quad u = \frac{x}{a}$

Differentiating [31] with respect to u:

$$dx = a\,du \qquad\qquad [32]$$

Substituting [31] and [32] into [30]:

$$\int \frac{1}{x^2 + a^2}\, dx \qquad\qquad [30]$$

$$= \int \frac{a}{a^2 u^2 + a^2}\, du \qquad\qquad [33]$$

$$= \frac{1}{a} \int \frac{1}{u^2 + 1}\, du \qquad\qquad [34]$$

$$= \frac{1}{a} \tan^{-1}(u) + c$$

Substituting [31] for u:

$$\int \frac{1}{x^2 + a^2}\, dx = \frac{1}{a} \tan^{-1}\left(\frac{x}{a}\right) + C \qquad\qquad [35]$$

We can now apply the result of [35] to [17] to solve for the configuration factor:

$$F_{d1-2} = \frac{z}{2\pi}\left[\int_0^b \left(\frac{1}{y^2 + z^2}\right) dy - \int_0^b \left(\frac{1}{(y^2 + a^2 + z^2)}\right) dy\right] \qquad\qquad [17]$$

Let: $\quad k^2 = a^2 + z^2 \qquad\qquad [36]$

$$F_{d1-2} = \frac{z}{2\pi}\left[\int_0^b \left(\frac{1}{x^2 + z^2}\right) dy - \int_0^b \left(\frac{1}{(x^2 + k^2)}\right) dy\right] \qquad\qquad [37]$$

$$= \frac{z}{2\pi}\left[\left|\frac{1}{z} \tan^{-1}\left(\frac{y}{z}\right) + C\right|_0^b - \left|\frac{1}{k} \tan^{-1}\left(\frac{y}{k}\right) + D\right|_0^b\right] \qquad\qquad [38]$$

where C and D are constants of integration

$$= \frac{z}{2\pi}\left[\left[\frac{1}{z} \tan^{-1}\left(\frac{b}{z}\right) + C\right] - \left[\frac{1}{z} \tan^{-1}\left(\frac{0}{z}\right) + C\right] - \right.$$

$$\left. \left[\frac{1}{k} \tan^{-1}\left(\frac{b}{k}\right) + D\right] + \left[\frac{1}{k} \tan^{-1}\left(\frac{0}{k}\right) + D\right]\right]$$

$$= \frac{z}{2\pi}\left[\frac{1}{z} \tan^{-1}\left(\frac{b}{z}\right) - \frac{1}{k} \tan^{-1}\left(\frac{b}{k}\right)\right] \qquad\qquad [39]$$

Substituting for k from [36]:

$$F_{d1-2} = \frac{z}{2\pi}\left[\frac{1}{z} \tan^{-1}\left(\frac{b}{z}\right) - \frac{1}{\sqrt{a^2 + z^2}} \tan^{-1}\left(\frac{b}{\sqrt{a^2 + z^2}}\right)\right] \qquad\qquad [40]$$

and rearranging for z:

$$F_{d1-2} = \frac{1}{2\pi}\left[\tan^{-1}\left(\frac{b}{z}\right) - \frac{z}{\sqrt{a^2+z^2}} \tan^{-1}\left(\frac{b}{\sqrt{a^2+z^2}}\right)\right]$$ [41]

To confirm the equation in Figure 2 it is now simply a matter of substituting $c = z$ changing to the variables X and Y established in the Figure. We have:

$$X = \frac{a}{b} \text{ and } Y = \frac{c}{b}$$

$$F_{d1-2} = \frac{1}{2\pi}\left[\tan^{-1}\left(\frac{b}{c}\right) - \frac{c}{\sqrt{a^2+c^2}} \tan^{-1}\left(\frac{b}{\sqrt{a^2+c^2}}\right)\right]$$ [42]

$$= \frac{1}{2\pi}\left[\tan^{-1}\left(\frac{1}{Y}\right) - \frac{Y}{\sqrt{X^2+Y^2}} \tan^{-1}\left(\frac{1}{\sqrt{X^2+Y^2}}\right)\right]$$ [43]

Limits

It is useful to consider the limiting behaviour of Equation [42] as c tends towards zero and infinity. These limits are solved directly by substitution:

$$\text{Lim}_{c\to0} F_{d1-2} = \frac{1}{4}$$ [44]

$$\text{Lim}_{c\to\infty} F_{d1-2} = 0$$ [45]

From [44] and the wing wall configuration factor algebra in Equation [2] of the parent document the received radiation flux at c = 0 will be one half of the emitted radiation flux.

However the situation is somewhat different for a return wall. From [44] and the wing wall configuration factor algebra in Equation [3] of the parent document the received radiation flux at c = 0 will be zero. These lower limits are not intuitively apparent, but they are borne out by the analytical solution and by modelling.

The upper limit at Equation [45] is intuitively apparent for both the wing and return wall.

Perhaps you can appreciate why most folk will defer to published tables of configuration factors for regular rectangular, cylindrical or spherical geometries.

Appendix B

FDS Modelling

The heat source was modelled as a 989.4°C radiator panel to produce a radiant heat flux of 144 kW/m^2 in accordance with Equation [1].

The computational domain was maintained as AIR with 40% humidity and FDS default values for ambient temperature, pressure and gravity. Initially air and water vapour were removed from the model in an attempt to simulate non-interacting media. Sensitivity analysis identified that the presence of air had no significant effect on the model.

Ambient temperature has no influence on the modelled results because measurements were confined to received radiation flux at an inert boundary.

Gravitational acceleration was maintained at the FDS default -9.81 m/s^2 in the Z direction.

The large eddy simulator was initially disabled (LES = .FALSE.) to reduce the computational burden as no significant media interactions were anticipated (or, through a study of velocity vectors, actually occurred) .

Ideally the modelled ambient pressure would have been reduced to zero to match the non-interacting media but this caused computational errors with the FDS pressure solver. Ambient pressure was therefore maintained at the default value of 101.3 kPa.

Arrays of DEVICES were used as radiometers at the source, the relevant boundary and 1 m beyond the relevant boundary to validate the analytical computation.

The FDS computational domain comprised a single mesh of 7.2 million 0.05 m cubic cells.

Cell size validation was completed by sensitivity analysis. Halving the cell dimensions made less than 0.5% difference in received radiation flux measurements.

The D*/dx parameter described in the FDS Users Guide is not valid where non-interacting media are defined. However with a default air atmosphere the D*/dx value for the mesh was 90 indicating a very fine mesh with adequate computational resolution (a value of between 4 and 16 is expected to produce adequate resolution for numerical computation).

The radiation solver was investigated by increasing the solid angular resolution from the default value of 104 to 4096 with parameters adjusted to require full resolution of radiation throughout the computational domain at each time step (refer to Section 9.4 of the FDS Users Guide). This improved the modelled results to within 1% of the analytical solution, but at a significant increase in computational burden. RADI parameters were finally run with an angular resolution of 1024 which proved to be a reasonable compromise between accuracy and computational time.

An initial estimate for the FDS solid angular resolution can be determined by calculation of the equivalent rectangular dimensions of the surface area of a sector of a hemisphere of radius equal to the maximum width or length of interest to the basic cell dimension. Insufficient solid angular resolution can be expected to result in fringing effects from the sides and corners of the radiator. The received radiation contribution from distant objects and objects viewed within a relatively acute solid angle cannot be expected to be accurately modelled and this will result in divergence from ideal behaviour.

The numerical precision of FDS has not been investigated in this study. The sum of a large number (order 10^4) of trigonometric functions, many at asymptotic limits, is expected to challenge numerical precision.

DEVICES in FDS from release 5.2 are calculated at the centre of a cell as opposed to the average of the eight surrounding cells (and that devices should be specified to lie on the computational grid). With a basic cell dimension of 1 unit, a DEVICE at location 0,0,0 will actually be measured at 0.5, 0.5, 0.5.

The computational domain was OPEN with the exception of the receiving plane.

The received radiation flux fields in the plane of the interest are presented in Figures B1 to B5. The radiating unprotected wall is on the right hand side of each image. Note that the contour colour for maximum received radiation has been adjusted for each image to better show the field distribution.
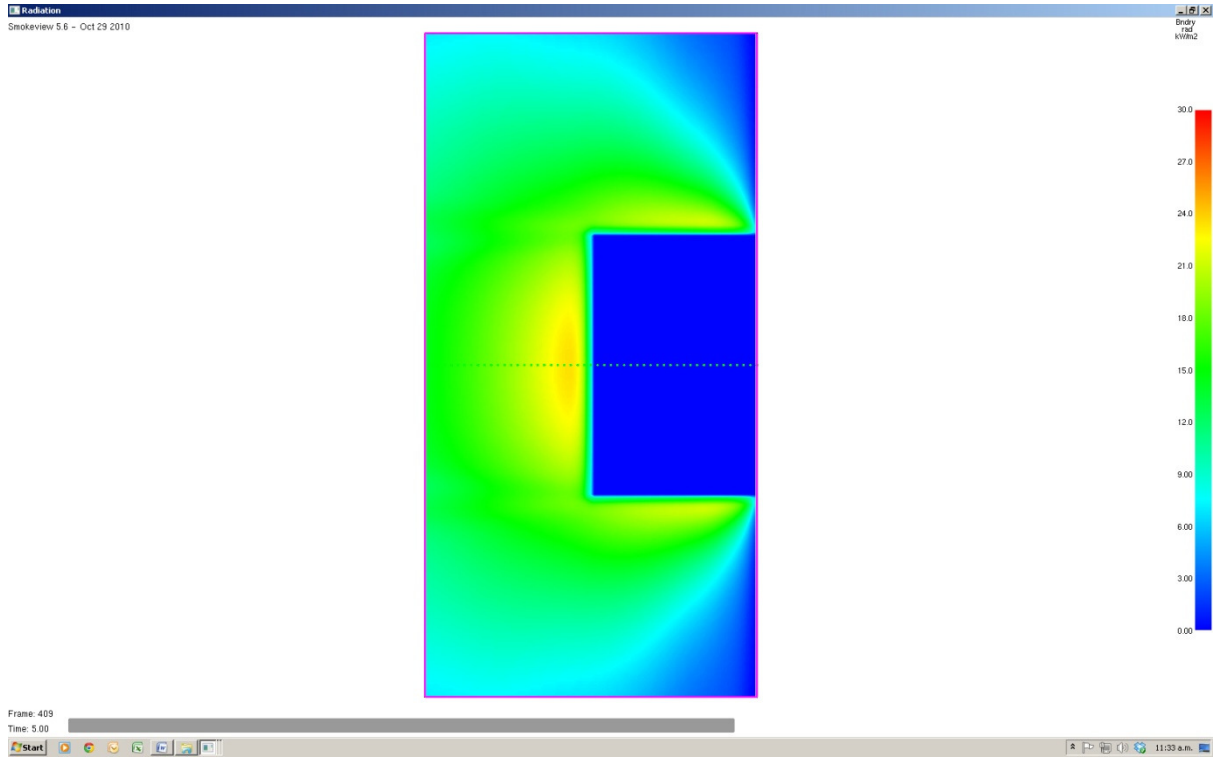
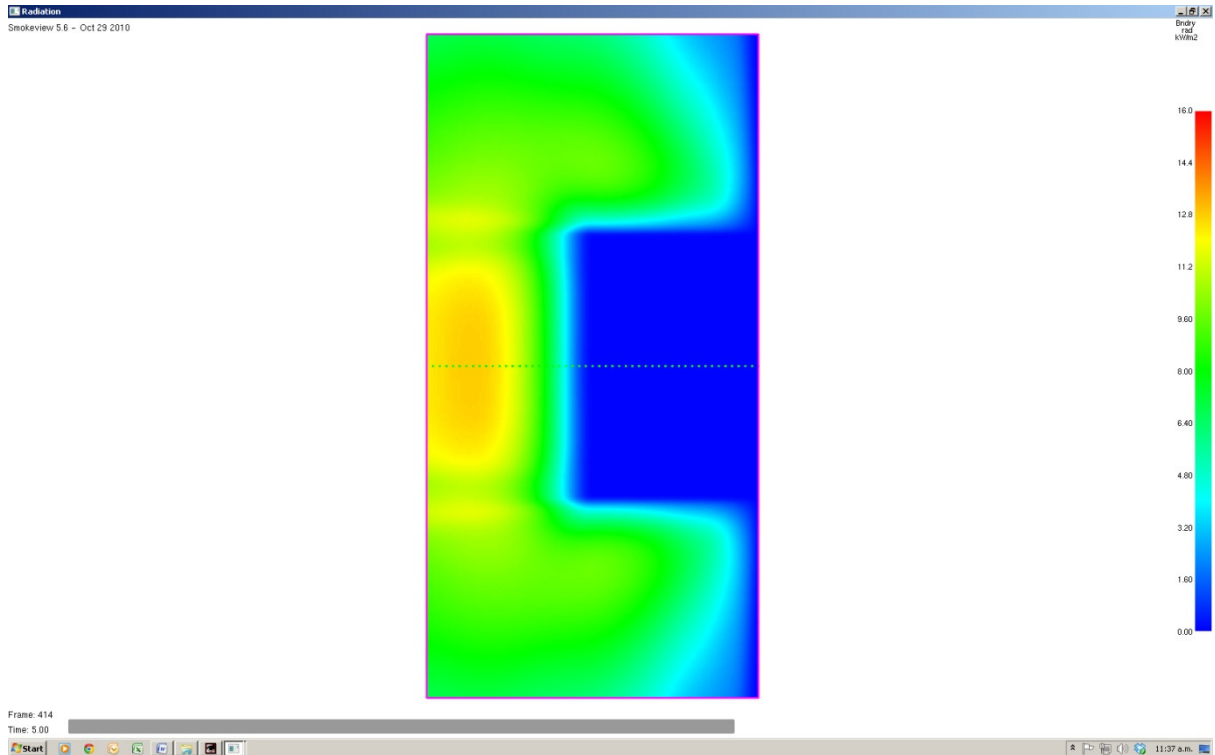Figure B1. Radiation Flux Field for Wing Wall at Boundary
(red contour is 30 kW/m^2)

Figure B2. Radiation Flux Field for Wing Wall 1 m Beyond Boundary
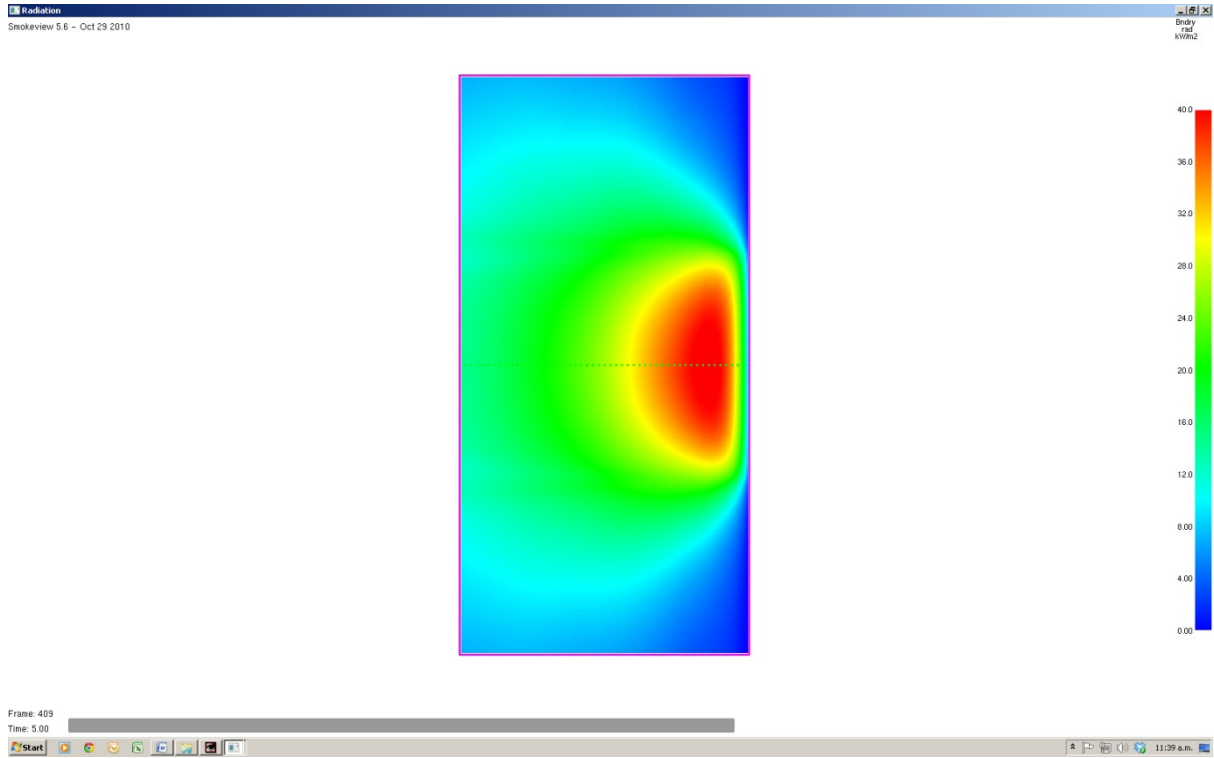(red contour is 16 kW/m^2)

Figure B3. Radiation Flux Field for Return Wall at Boundary
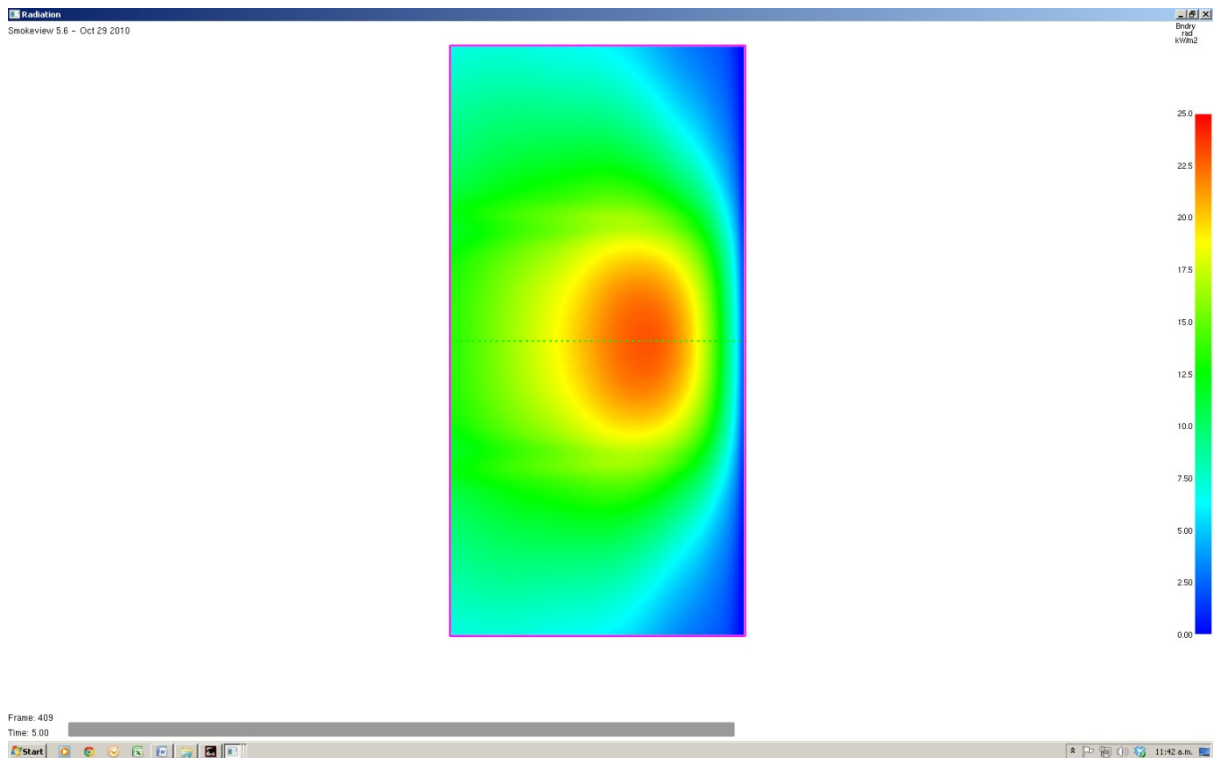(red contour is 40 kW/m^2)

Figure B4. Radiation Flux Field for Return Wall 1 m Beyond Boundary
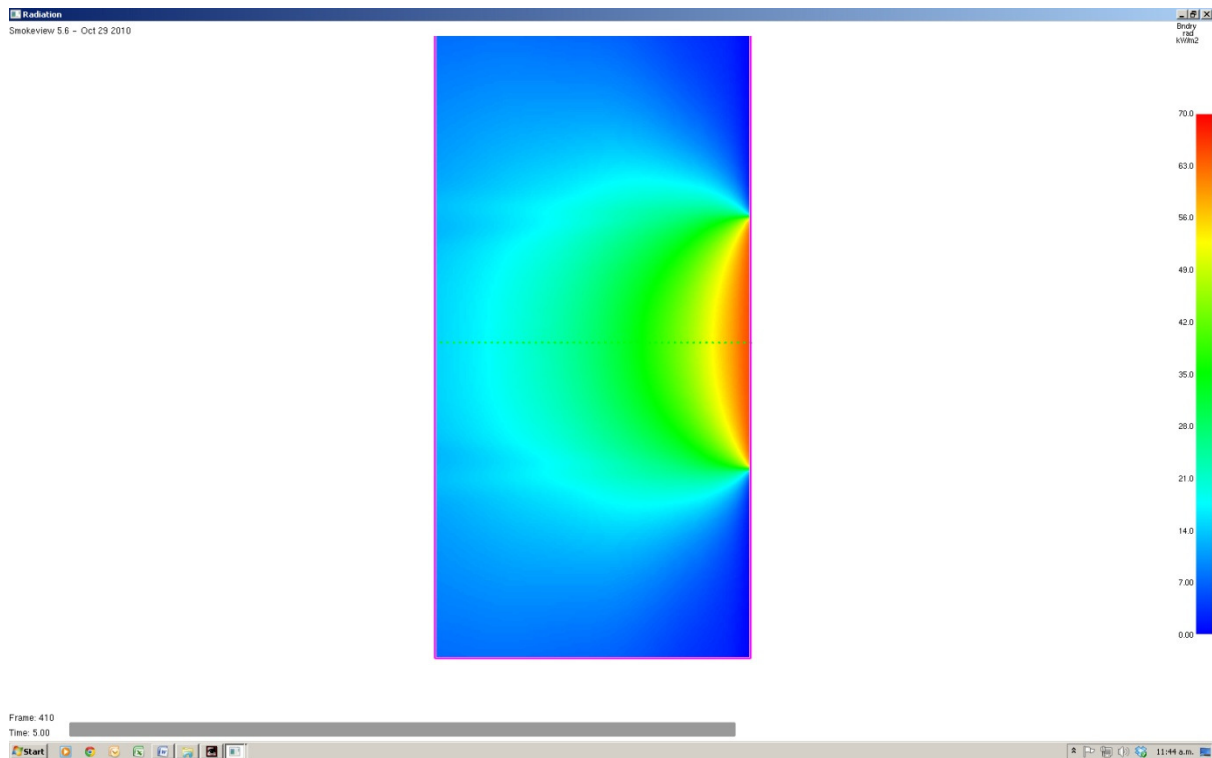(red contour is 25 kW/m^2)

Figure B5. Radiation Flux Field for no Wing or Return Wall at Boundary
(red contour is 70 kW/m^2)

The FDS general model for this study is listed below. To aid brevity all DEVICES are not listed. Each simulation varied only in the placement of the radiating panel and the wing wall. The wing wall OBSTRUCTION was incorporated in the wing wall models to show the effect of radiation shielding at and 1 m beyond the relevant boundary as shown in Figures B1 and B2.

For the case of a wing wall at the boundary it was necessary to ascribe a thickness to the wall to show the effect of radiation shielding. The wall was defined with a thickness of 0.05 m to align with the dimension of computational grid. The wall thickness produced penumbra fringing at the edges of the wing wall (Figure B1) which reduced the peak received radiation flux at the boundary.   For the analytical case of an infinitely thin wing wall the received radiation flux shown in Figure B5 can be simply truncated to zero over the area of the wing wall.

Although the model is deceptively simple the defined solid angle resolution and the size of the computational domain can be expected to result in run times up to two hours to achieve five seconds of simulated time on a dedicated 3.9 GHz i7 processor with 16 GB of RAM and a 64 bit operating system running an OpenMP multiprocessor FDS compilation.

```
&HEAD  CHID = 'Radiation', TITLE = 'Radiation Study'/

/Set Operating Environmental Variable 'OMP_STACKSIZE = 200M' in W7 to allocate RAM

&MESH  ID = 'Mesh1', IJK = 100,360,200, XB = 0,5,0,18,0,10/

&MISC  SURF_DEFAULT = 'INERT'
       RESTART = .FALSE.

&RADI  NUMBER_RADIATION_ANGLES = 1024/ TIME_STEP_INCREMENT = 1, ANGLE_INCREMENT = 1,

&TIME  T_END = 5/

&SURF  ID = 'PANEL', COLOR = 'RED', TMP_FRONT = 989.4, EMISSIVITY = 1/

/Radiating Panel
/Change Y dimensions to 0,16.5 for exposed wall at boundary
/Change Y dimensions to 0.4,16.9 for 0.4 m Return Wall
&OBST  XB = 0,0,1,17.5,3,7
       SURF_ID6 = 'INERT','PANEL','INERT','INERT','INERT','INERT'
        BNDF_OBST = .FALSE./

/Wing Wall (only used in consideration of Wing Wall to 1 m beyond boundary)
&OBST  XB = 0,2.5,1,1,3,7, BNDF_OBST = .FALSE./

/MESH 1 Boundaries
&VENT  XB = 0,5,18,18,0,10, SURF_ID = 'OPEN'/
&VENT  XB = 0,0,0,18,0,10, SURF_ID = 'OPEN'/
&VENT  XB = 5,5,0,18,0,10, SURF_ID = 'OPEN'/
&VENT  XB = 0,5,0,18,10,10, SURF_ID = 'OPEN'/
&VENT  XB = 0,5,0,18,0,0, SURF_ID = 'OPEN'/

&DEVC  XYZ = 0,9.6,5, QUANTITY = 'RADIATIVE HEAT FLUX', IOR = 1, ID = 'Source RAD'/

/Boundary Devices
&DEVC  XYZ = 0.1,0,5, QUANTITY = 'RADIATIVE HEAT FLUX GAS', ORIENTATION = 0,1,0, ID = '0.1 BRAD'/
&DEVC  XYZ = 0.2,0,5, QUANTITY = 'RADIATIVE HEAT FLUX GAS', ORIENTATION = 0,1,0, ID = '0.2 BRAD'/

        /&DEVC …. To complete linear array

&DEVC  XYZ = 4.8,0,5, QUANTITY = 'RADIATIVE HEAT FLUX GAS', ORIENTATION = 0,1,0, ID = '4.8 BRAD'/
&DEVC  XYZ = 4.9,0,5, QUANTITY = 'RADIATIVE HEAT FLUX GAS', ORIENTATION = 0,1,0, ID = '4.9 BRAD'/

&BNDF  QUANTITY = 'RADIATIVE HEAT FLUX'/

&TAIL/
```

Appendix C

Graphics Overlays

The following overlays are provided for qualitative comparison between the analytical and modelled received radiation flux. Colours have been preserved from the original analysis to ease identification. The FDS results are shown as dashed curves. Note that vertical scales have been increased to improve visual resolution while retaining maximum values.
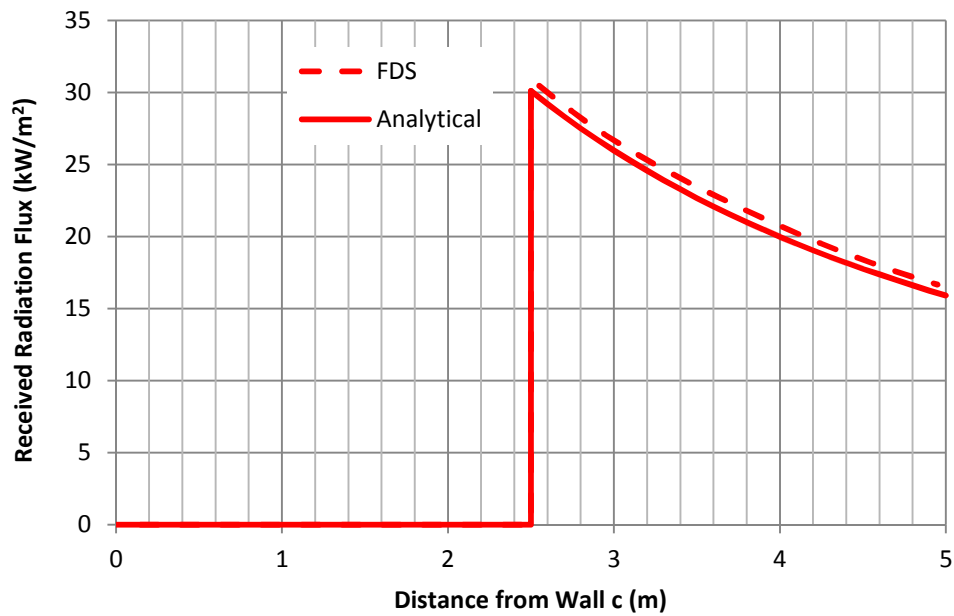

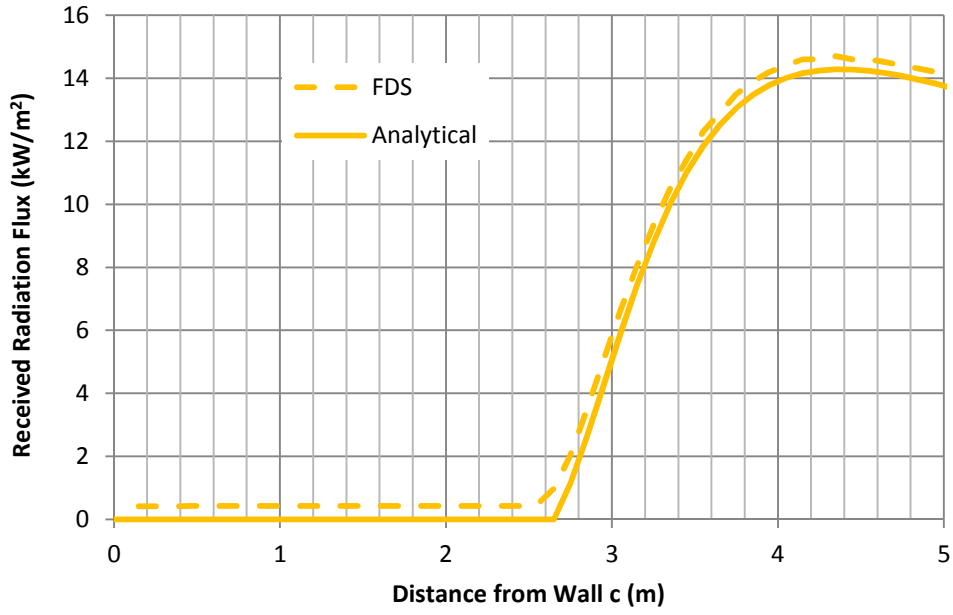Figure C1. 2.5 m Wing Wall at the Boundary
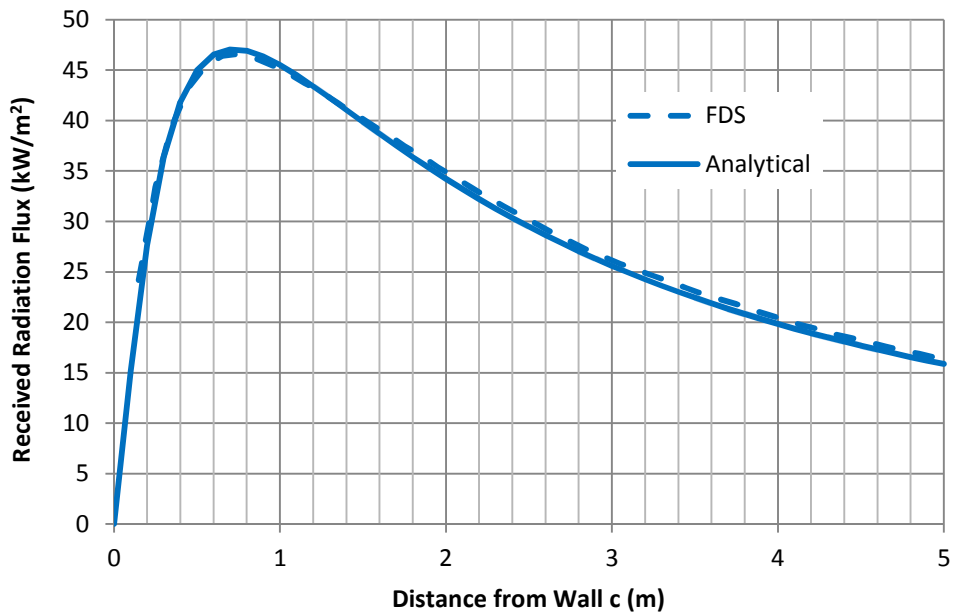
Figure C2. 2.5 m Wing Wall 1 m Beyond the Boundary

Figure C3. 0.4 m Return Wall at the Boundary
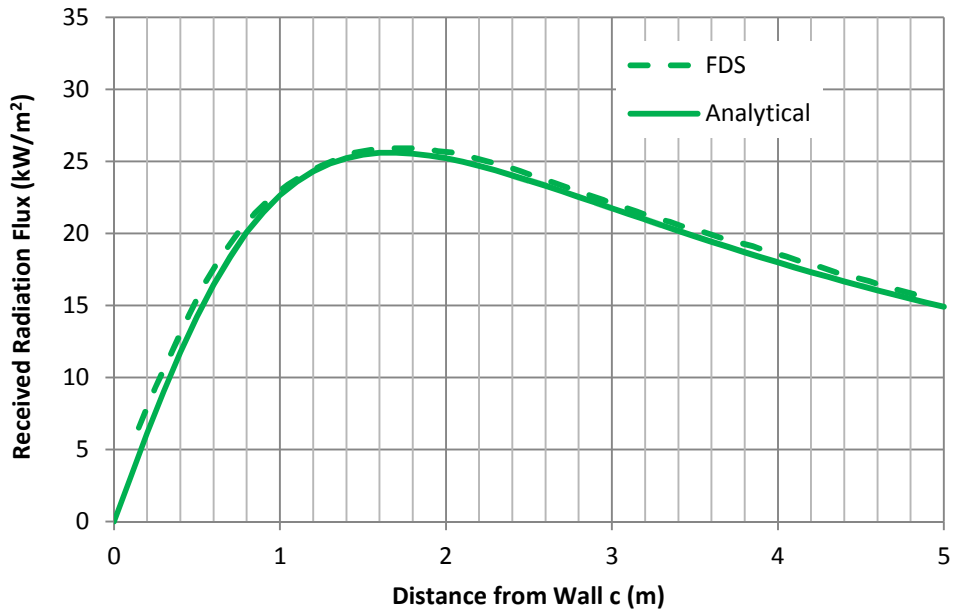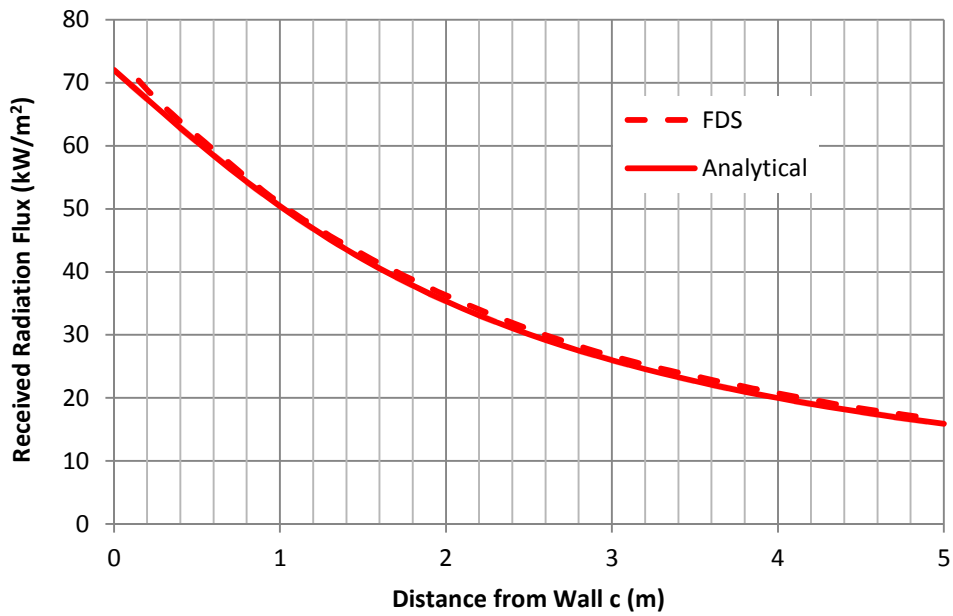
Figure C4. 0.4 m Return Wall 1 m Beyond the Boundary

Figure C5. No Wing/Return Wall at the Boundary

Appendix D

FireWind Study

Spatial received radiation flux was calculated using a single rectangular Z plane emitter 16.5 m long and 4 m high at a temperature of 989°C (corresponding to an emitted radiation flux of 144 kW/m^2). The emitter was placed on and 1 m away from the plane of the elemental area (defined in RADIATION as the point P).

The resolution of the received radiation map is dictated by the map scale factor. For total spatial distribution this was set at 5 m. In order to provide comparable results to FDS and analytical experiments the map scale factor was reduced to 0.4 and the point P was stepped from 0.2 m to 4.8 m in 0.4 m increments.

Figure D1 shows the spatial maximum received radiation flux for a radiating wall at the boundary (without a wing or return wall). Although the magnitude of the received radiation flux is greater than the analytical or FDS modelled solutions(explained in the parent text) the radiation contours correspond with the comparable FDS study shown in Figure B5.

Figure D2 shows the spatial maximum received radiation flux for 1 m beyond the boundary. As with the previous analysis, the radiation contours correspond with the comparable FDS study shown in Figure B4.
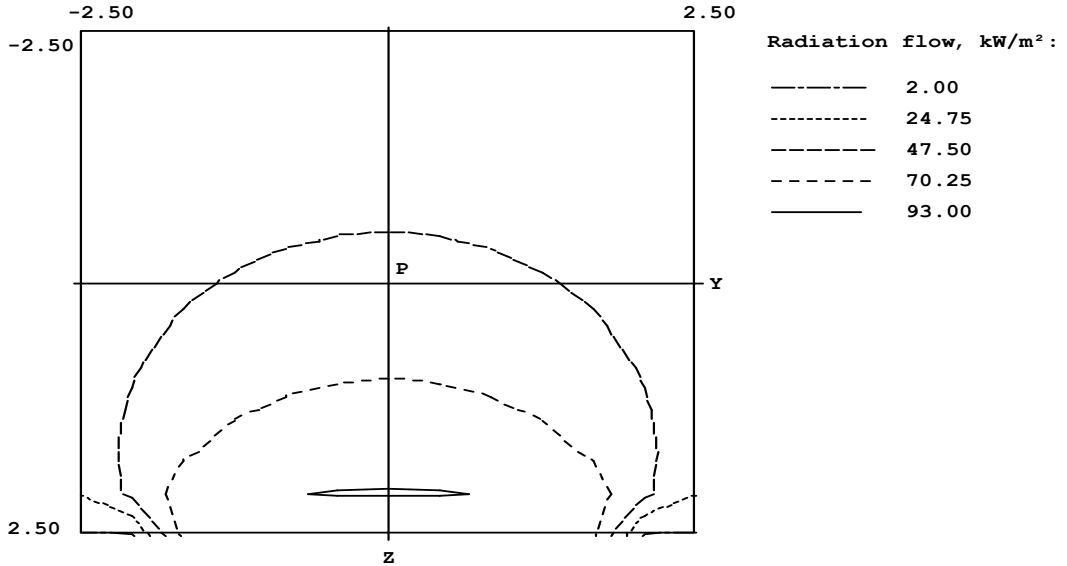
Program Radiation

(All dimensions are in meters)
Z-sources:
Radiation temperature 989°°

Distance	Offset		Size of source		Opening
Z	Xz	Yz	X	Y	%
2.5	8.25	0	16.5	4	100

RADIATION MAP YZ

Radiation flow, kW/m²:

—·—·— 2.00
---------- 24.75
— — — — 47.50
– – – – – 70.25
————— 93.00

Nodal radiation data, kW/m²:

Z \ Y	-2.50	-1.25	0.00	1.25	2.50
-2.50	25.60	29.37	30.82	29.37	25.60
-1.25	30.38	37.12	39.81	37.12	30.38
0.00	35.60	48.75	54.00	48.75	35.60
1.25	37.97	67.76	76.34	67.76	37.97
2.50	0.000	71.93	71.93	71.93	0.000

Orientation of maximum radiation flow
at point P(0,0,0): $\theta = 33.8°$, $\varphi = 0.0°$

Figure D1. FireWind Maximum Received Radiation Flux at the Boundary
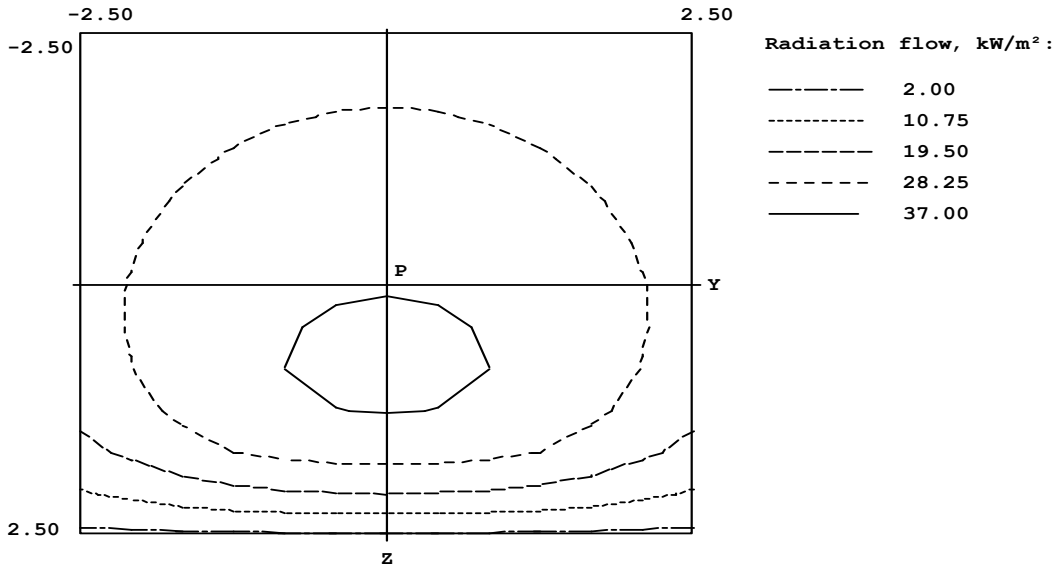with no Wing or Return Wall

Program Radiation

(All dimensions are in meters)
Z-sources:
Radiation temperature 989°°

Distance	Offset		Size of source		Opening
Z	Xz	Yz	X	Y	%
2.5	9.25	0	16.5	4	100

RADIATION MAP YZ

Radiation flow, kW/m²:

—·—·—   2.00
----------   10.75
— — — —   19.50
- - - - -   28.25
————   37.00

Nodal radiation data, kW/m²:

z \ Y	-2.50	-1.25	0.00	1.25	2.50
-2.50	21.29	24.14	25.23	24.14	21.29
-1.25	23.99	28.69	30.55	28.69	23.99
0.00	25.59	33.45	36.62	33.45	25.59
1.25	21.70	33.20	37.33	33.20	21.70
2.50	0.000	0.000	0.000	0.000	0.000

Orientation of maximum radiation flow
at point P(0,0,0): $\theta = 46.2°, \varphi = 0.0°$

Figure D2. FireWind Maximum Received Radiation Flux 1 m Beyond
the Boundary with no Wing or Return Wall